Journal of the European Ceramic Society 19 (1999) 2415–2419

PII: S0955-2219(99)00101-6
0955-2219/99/$ - see front matter

Titanium Carbide Based Composites for High Temperature Applications

Nuri Durlu

Materials and Chemical Technologies Research Institute, Marmara Research Center, Tübitak Gebze, Kocaeli, Turkey

Abstract

Titanium carbide based composites with nickel alloys and iron alloys are currently used in high performance applications where wear and corrosion are the main sources of material failure. For high temperature critical applications, however, the metallic binders nickel and iron limit the use of TiC-based composites. Hence, new binder systems which have good high temperature properties need to be developed in order to extend the use of TiC-based composites. Silicides and aluminides are potential binder systems with their good high temperature corrosion and mechanical properties. In this study, two binder systems, Fe–25 at% Si and Fe–40 at% Al have been selected, and were processed with reaction sintering of elemental Fe and Si, or Fe and Al powders, with 65 wt% TiC and 80 wt% TiC powders at temperatures at around 1410–1430°C under vacuum. X-ray diffraction analysis show TiC and Fe_3Si phases in the TiC-iron silicide composites, whereas TiC, Fe_3Al_2 and $Fe_3AlC_{0.5}$ phases were observed in TiC–iron aluminide composites. Differential thermal analysis of the samples shows that liquidus temperatures of the iron-silicide and iron-aluminide binders were around 1265 and 1425°C, respectively. Vickers microhardness values of 1100–1470 kg mm^{-2} and 3-point bending strengths of 600–775 MPa were obtained in these high density reaction sintered TiC–iron silicide and TiC-iron aluminide composites. © *1999 Elsevier Science Ltd. All rights reserved.*

Keywords: binder phases, reaction sintering, TiC, composites, mechanical properties

1 Introduction

The high melting point (3065°C), and the low density (4·93 g cc^{-1}) of TiC, makes it a potential material for high temperature applications. Monolithic TiC, however, is brittle at ambient temperatures, and metals such as Ni, Co, and Fe have been incorporated as a ductile second phase to improve its fracture toughness. Liquid phase sintering, and melt infiltration are the two common production techniques used in the processing of these materials. Nickel is the most commonly used metallic binder phase in TiC based composites, which is mainly due to the low wetting angle, 30° under vacuum (10^{-5} torr) at 1450°C,[1] that liquid Ni forms with solid TiC. Addition of molybdenum to nickel reduces the wetting angle with TiC to zero,[1] and this leads to TiC-based composites with very good mechanical properties.

In the 1950s considerable effort had been devoted to the development of TiC-based composites for high temperature critical applications such as turbine blades.[2,3] The major binder metallic alloys being investigated were: Ni–Mo, Ni–Mo–Al, Ni–Cr, and Ni–Co–Cr.[3] These systems, however, were not able to meet the high temperature requirements, such as high strength, oxidation resistance and ductility, and TiC-based composites found use in less critical applications such as cutting tools and metal working tools.[3]

In the 1980s, ordered intermetallic compounds, especially nickel aluminides (Ni_3Al, NiAl), titanium aluminides (Ti_3Al, TiAl, $TiAl_3$), and iron aluminides (Fe_3 Al, FeAl), have been considered as potential high temperature materials. This is mainly due to the properties that these intermetallics possess, such as increase in strength with temperature, relatively low density, and good oxidation resistance. The research efforts on aluminides were successful, and in the 1990s two of these aluminides, Ni_3Al and TiAl, are commercialized as high temperature materials for critical components.[4]

Recently, intermetallic aluminides have also been utilized as binder phase in the preparation of TiC-based composites.[5–9] Hot pressing and presureless melt- infiltration techniques were utilized for the processing TiC-Ni_3Al[5,6] and TiC-FeAl[7–9] composites with promising mechanical properties comparable to that of commercially available TiC–Ni and WC–Co cermets.[6,10] Of these intermetallic aluminide composites, TiC–Ni_3Al composites might be used

for high temperature (~1100°C) applications,[6] and TiC–FeAl composites can be used under more severe corrosion conditions.[7–10] Intermetallic aluminides have also been used as binder phase in the processing of other carbides, oxides, and borides, such as WC–Ni_3Al and Al_2O_3–Ni_3Al,[5] Al_2O_3–(Ti,Fe,Nb,Mo,Zr,Ni) aluminides of different stoichiometry,[11] WC–FeAl, TiB_2–FeAl and ZrB_2–FeAl,[12] Al_2O_3–$NbAl_3$[13] and Al_2O_3–FeAl.[14]

Hot pressing and pressureless infiltration techniques have been used in the processing of TiC–Ni_3Al and TiC–FeAl composites.[6–9] An alternative processing technique for the production of TiC-based intermetallic composites is the reactive sintering technique. This sintering technique has been successfully applied for the processing of high density Al_2O_3–aluminide composites starting with metal oxide and Al powders and their in-situ synthesis,[11,13] as well as for the processing of high density Al_2O_3–FeAl composites, starting with Al_2O_3 , elemental Al, and Fe powders, and their in-situ synthesis at 1450–1500°C.[14]

In this study, the possibility of using pressureless reaction sintering technique is investigated for the processing of TiC–Fe_3Si and TiC–FeAl composites, which contain 65 wt% TiC and 80 wt% TiC. The TiC–Fe_3Si is a new composite system, and has been selected due to the very good corrosion properties of Fe_3Si.[15] The composites TiC–FeAl had already been processed with melt infiltration technique,[7–9] and in this study reaction sintering technique is utilized as an alternative technique for the processing of these composites.

2 Experimental Procedure

Commercially available powders of Al (Merck, Germany), Fe (Poudmet, France), Si (Alfa, USA), and high vacuum grade TiC (H.C. Starck, Germany) were used in this study. Powder mixtures of Fe–25 at% Si, (abbreviated as Fe25Si in the text) and Fe–40 at% Al (abbreviated as Fe40Al in the text) were attritor milled (Union Process, USA) with varying contents of TiC (65 and 80 wt%) in a stainless steel container for 2 h. In the preparation of powder mixtures, WC balls with 4·7625 mm. diameter were used for the TiC–Fe25Si composites, and stainless steel balls were used for the TiC–Fe40Al composites. Ethyl alcohol was utilized as milling solution. The ball weight to powder weight ratio was 20 for TiC–Fe25Si composites and 10 for TiC–Fe40Al during milling operations. The powder mixtures were dried under vacuum at 80°C. The samples were cold isostatically pressed to pellets of approximately 19 mm in diameter under a pressure of 250 MPa, and then sintered under vacuum ($< 10^{-1}$ torr) in a vacuum furnace (Model Rotovac II, Centorr/Vacuum Industries, USA) with graphite heating elements, for 60 min at the sintering temperature. High purity alumina plates were used as substrate during the experiments. After sintering, the densities of the samples were measured picnometer (Model 1320, Micromeritics, USA). The samples were cut, ground and polished with diamond paste, and examined with optical microscope and scanning electron microscope (Model JXA-840A, Jeol, Japan). X-ray diffraction data was obtained by a computer controlled diffractometer (Model XRD-6000, Shimadzu, Japan) where Cu K_α was used as X-ray beam source. Differential thermal analysis (Model 92-16.18, Setaram, France) measurements were made in alumina crucibles upto 1500°C, with a heating rate and cooling rate of 20°C min^{-1} under argon. Calibration check of DTA equipment was made with high purity nickel. Vickers hardness measurements (Leitz, Germany) was made under 500 g load with a dwell time of 30 s.

3 Experimental Results and Discussion

3.1 Powder morphology and size

In Fig. 1 scanning electron microscopy (SEM) images of the as received powders are given. The Al powder has flaky morphology [Fig. 1(a)]. Iron powder has spherical morphology with average particle size less than 5 microns [Fig. 1(b)]. In the as received Si (< -325 mesh) and TiC powders (Fischer sub seive size 4 microns), small particles (< 10 microns), as well as big particles of about 15–20 microns was also observed [Fig. 1(c) and Fig. 1(d)].

3.2 Sintering and phase stability

Sintering experiments were performed under vacuum ($< 10^{-1}$) for 1 h at the sintering temperature and then furnace cooled. A summary of the X-ray diffraction data obtained from the polished surfaces of the TiC–Fe25Si and TiC–Fe40Al composites are given in Table 1. The lattice parameter of the as received TiC powder and the lattice parameter of the TiC phase in the samples was calculated from the (422) reflection. Low order reflections (220) and (110) had been used in calculating the lattice parameters of Fe_3Si and $Fe_{0.6}Al_{0.4}$ (abbreviated as Fe_3Al_2 in the text) phases, respectively. The calculated lattice parameter of the phase Fe_3Al_2 was found to be very close to the JCPDS card value, whereas the lattice parameter of the phase Fe_3Si was found to be greater than the card value. After sintering of TiC-iron silicide composites about 1·5–2 wt% loss was observed in the

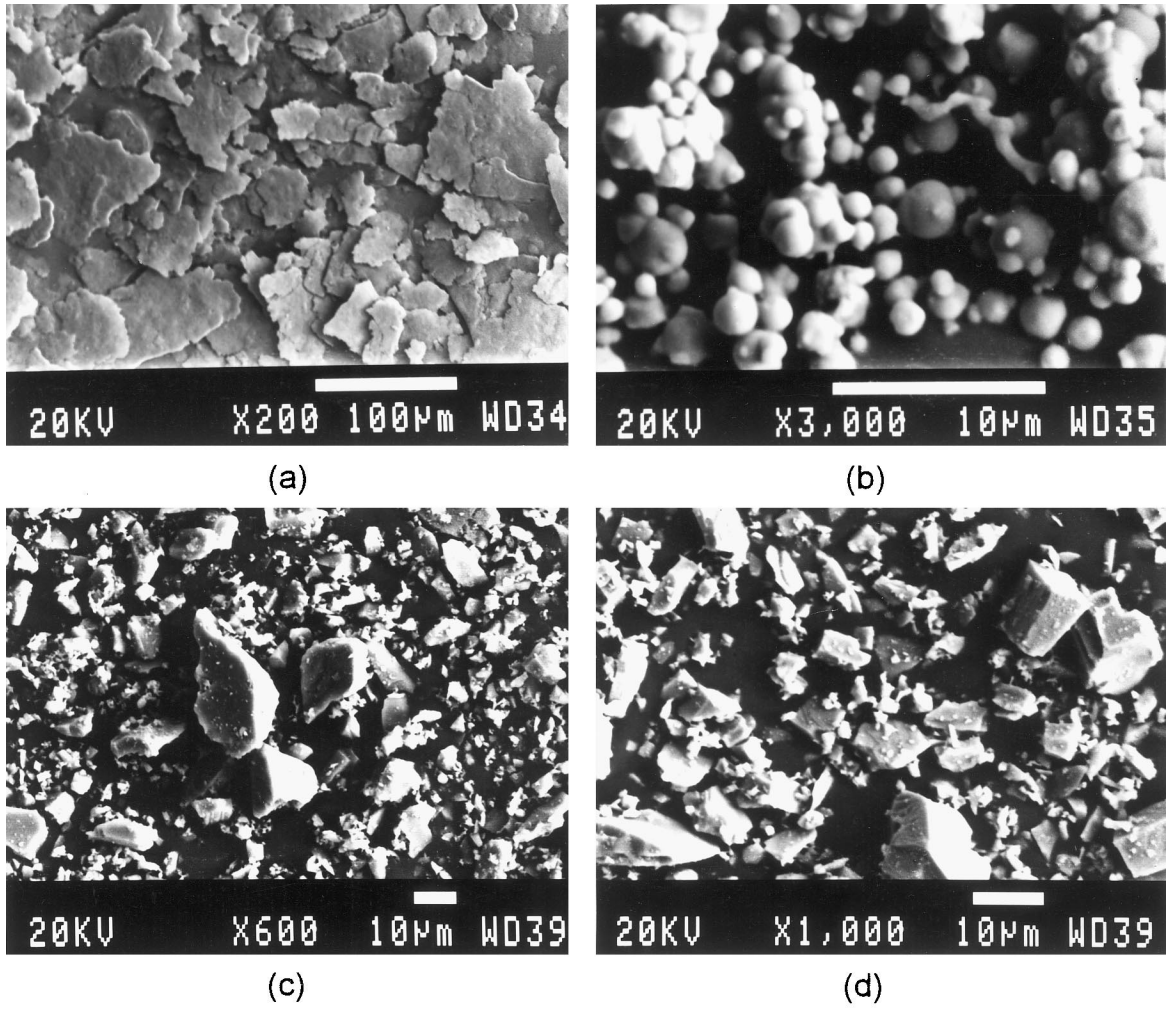

Fig. 1. Secondary electron images of the powders used in reaction processing of TiC–iron silicide and TiC–iron aluminide composites: (a) Al, (b) Fe, (c) Si, (d) TiC.

Table 1. Major phases observed by X-ray diffraction in TiC–Fe25Si and TiC–Fe40Al composites and their lattice parameters[a]

Sample	*Phases*	*Lattice parameter (A°)*
Fe25Si–80% TiC	TiC	$a = 4{\cdot}3232$
	Fe_3Si	$a = 5{\cdot}6715$
Fe25Si–65%TiC	TiC	$a = 4{\cdot}3238$
	Fe_3Si	$a = 5{\cdot}6695$
Fe40Al–80%TiC	TiC	$a = 4{\cdot}3228$
	Fe_3Al_2	$a = 2{\cdot}9014$
	$Fe_3AlC_{0{\cdot}5}$ (minor)	$a = 3{\cdot}77$
Fe40Al–65%TiC	TiC	$a = 4{\cdot}3248$
	Fe_3Al_2	$a = 2{\cdot}9018$
	$Fe_3AlC_{0{\cdot}5}$ (minor)	$a = 3{\cdot}77$
JCPDS #32-1383	TiC	$a = 4{\cdot}3274$
	TiC (as received)	$a = 4{\cdot}3282$
JCPDS #45-1207	Fe_3Si	$a = 5{\cdot}6533$
JCPDS #45-982	$Fe_{0{\cdot}6}Al_{0{\cdot}4}$	$a = 2{\cdot}8967$
JCPDS #29-44	$Fe_3AlC_{0{\cdot}5}$	$a = 3{\cdot}77$

[a]Samples were sintered at 1410 and 1430°C under vacuum for 1 h, respectively.

samples. Hence, the increase in the lattice parameter can be related to the deviation from the exact stoichiometry of the phase Fe_3Si, which has a wide range of compositional stability.[16] A slight reduction in the lattice parameter of TiC was also observed in all the samples (Table 1), and this reduction might be attributed to the change of the stoichiometry of TiC_{1-x} by C diffusion to the matrix during sintering. This is supported by the observation of a minor phase, $Fe_3AlC_{0{\cdot}5}$, in TiC–Fe40Al composites. This phase had also been observed previously in a mechanically alloyed iron aluminide with a composition Fe–35 at% Al–1·9 at% C, as fine dispersoids in the FeAl matrix.[17] It is likely that C diffusion from TiC during sintering lead to the formation of $Fe_3AlC_{0{\cdot}5}$.

The DTA cooling curves of the sintered TiC–Fe25Si and TiC–Fe40Al composites were used to determine the solidification temperatures of the phases Fe_3Si and Fe_3Al_2. In the sample Fe25Si–65%TiC, a major exothermic peak was observed in between 1235 and 1265°C, and this was correlated to the formation of Fe_3Si phase from the liquid upon solidification. Similarly, the DTA cooling curve of the sample Fe40Al–65%TiC shows a major exothermic peak which starts at around 1425°C, and this was related to the formation of the Fe_3Al_2 phase from the liquid phase. These two temperatures, i.e., 1265°C and 1425°C, correspond

to the liquidus temperatures of the Fe_3Si and Fe_3Al_2 phases within $\pm 5°C$ of the equilibrium values given in the binary Fe–Si[16] and Fe–Al[18] phase diagrams.

3.3 Microstructure, density, and microhardness

Backscattered electron micrograph of the reaction processed Fe25Si–65%TiC sample, is given in Fig. 2. The TiC (dark phase) has a relatively uniform distribution in the binder phase Fe_3Si (gray phase). The density of the sample was measured to be around ~99% theoretical density, which is consistent with the very little porosity observed in the microstructure. Increase in TiC content to 80%, lead to lower theoretical density of about 95%, with considerable amount of porosity observed in the microstructure. The amount of the binder phase, Fe_3Si, in the sample Fe25Si–80%TiC is about 14·5 vol%, which seems to be insufficient for obtaining high density samples under these experimental conditions.

Secondary electron micrograph of the reaction processed Fe40Al–65%TiC sample show a uniform distribution of TiC particles in the binder phase Fe_3Al_2 (Fig. 3). The sintered density of the Fe40Al–65%TiC and Fe40Al–80%TiC samples was measured to be greater than 98% theoretical density. In the processing of TiC–iron aluminide composites, especially for high TiC content (> 65 wt%), melt infiltration technique has been shown to be an effective technique for the achievement of high densities.[7–9] Liquid phase sintering technique, where TiC powders (2–3 μm) and FeAl powders (≈40 μm) were used, has also been tried for the processing of TiC–iron aluminide composites with high TiC content (> 65 wt%), but with little success.[9] The results of our study show that, reaction sintering technique, where elemental Fe and Al powders were used, lead to high density TiC–FeAl composites with TiC contents greater than 65 wt%.

The results of the density measurements and Vickers hardness measurements of the sintered TiC–Fe25Si and TiC–Fe40Al samples are given in Table 2. The sample, Fe25Si–65%TiC has a remarkably high Vickers microhardness value, 1469 kg mm^{-2}, and this can be related to the high density achieved by reaction sintering technique. The Vickers microhardness values of the reaction sintered TiC–FeAl samples (Table 2) was found to be less than the composites obtained by melt infiltration technique, which had been reported to be 1297 and 1778 kg mm^{-2} for the Fe40Al–65%TiC and Fe40Al–82·2%TiC composites, respectively.[7]

Some preliminary three-point bending tests (span length 25·4 mm) of the as sintered TiC–iron silicide and TiC–iron aluminide specimens (5×7×35 mm) were also done with a cross-head speed of 2 mm min^{-1}. The bending strengths of the samples are given in Table 2. In comparison to the 3-point bending strength (1034 MPa) obtained by Subramanian *et al.*[7] in melt infiltrated Fe40Al–65%TiC sample, the bending strength of reaction sintered Fe40Al-65%TiC was found to be around 750 MPa. At the present time the reasons of this difference are not clear, but one possible explanation is the formation of the brittle third phase, $Fe_3AlC_{0.5}$, observed in this sample (Table 1). Fracture surface analysis of the samples show that, TiC particles (dark phase) are surrounded by the iron-aluminide ligaments (white phase) (Fig. 4), which had been stated to increase the fracture toughness of TiC–FeAl composites.[9]

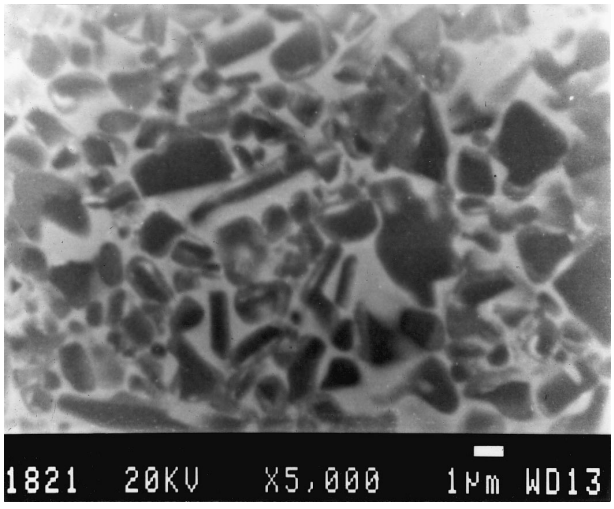

Fig. 2. Backscattered electron image of the high density Fe25Si–65%TiC sample obtained by reaction processing of elemental Fe and Si powders with TiC at 1410°C under vacuum for 60 min.

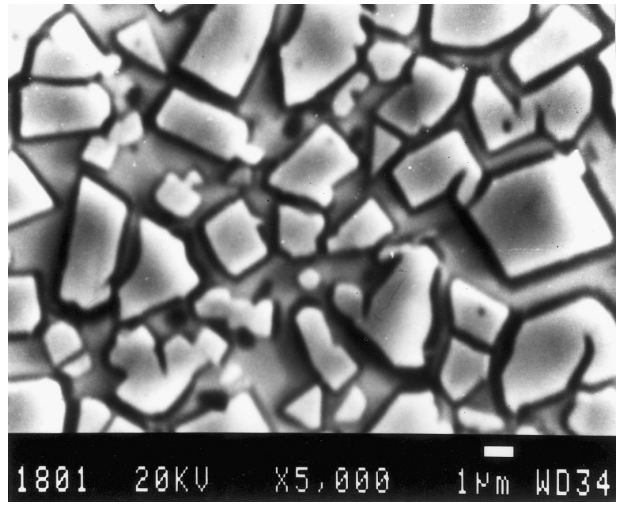

Fig. 3. Secondary electron image of the high density Fe40Al–65%TiC sample, obtained by reaction processing of elemental Fe and Al powders with TiC at 1430°C under vacuum for 60 min showing uniformly distributed TiC particles in the binder phase Fe_3Al_2. The sample was etched with 10% Nital followed by etching in Murakami solution.

Table 2. Mechanical property data of TiC–iron silicide composites and TiC–iron aluminide composites

Sample	*Density (%)*	*Hardness (kg mm^{-2})*	*Bend strength (MPa)*
Fe25Si–65%TiC	99	1469	767 ± 52[a]
Fe25Si–80%TiC	96	1257	596 ± 42
Fe40Al–65%TiC	98	1133	725 ± 45
Fe40Al–80%TiC	98	1460	595 [b]

[a] Error bars were given for five samples.
[b] Average of two tests

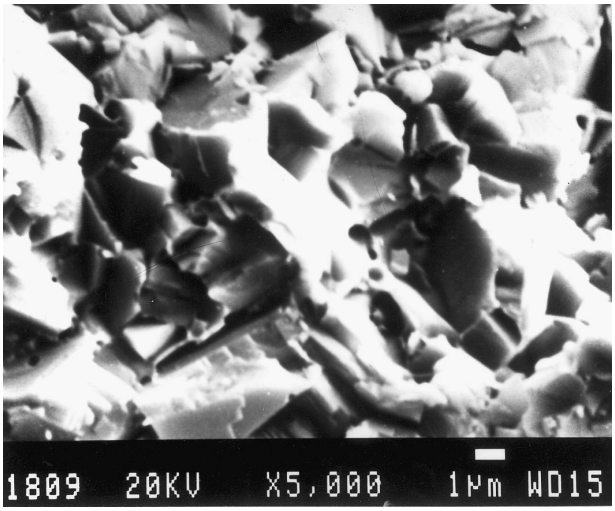

Fig. 4. Secondary electron image of the fracture surface of the sample Fe40Al–65%TiC, which shows TiC particles (dark phase) surrounded by the binder phase, Fe_3Al_2, bridging ligaments (bright phase).

4 Conclusions

1. High density TiC–iron silicide and TiC–iron aluminide composites, have been prepared by reaction sintering of elemental powders (Fe and Si, or Fe and Al) with TiC at temperatures 1410 and 1430°C, respectively.
2. In the reaction sintered Fe25Si–65%TiC, and Fe25Si–80%TiC samples, TiC and Fe_3Si were the major phases observed by X-ray diffraction.
3. In the reaction sintered Fe40Al–65%TiC and Fe40Al–80%TiC samples, besides the major phases TiC and Fe_3Al_2, a third minor phase $Fe_3AlC_{0.5}$ had also been observed by X-ray diffraction.
4. High hardness (1100–1470 kg mm^{-2}) with moderate bending strengths (600–750 MPA) were achieved in reaction sintered TiC–iron silicide and TiC–iron aluminide composites.

Acknowledgements

This research was supported by NATO under grant SFS-TU-POWMETAL. Experimental assistance of Mr Hidayet Bodur and Mr Rasim Işik is gratefully acknowledged. Thanks are also due to members of Materials Research Division for their help at various stages of this work.

References

1. Humenik, M. and Parikh, N. M., Cermets: I, fundamental concepts related to microstructure and physical properties of cermet systems. *J. Am. Ceram. Soc*., 1956, **39**(2), 60–63.
2. Lenel, F., Powder Metallurgy Principles and Applications. *Metal Powder Industries Federation*, Princeton, N J, 1980.
3. Goetzel, C. G., Cermets, *ASM Handbook*, Vol. 7. American Society for Metals, OH, 1993, pp. 799–815
4. Subramanian, P. R., Mendiratta, M. G. and Dimiduk, D. M., Advanced intermetallic alloys—beyond gamma titanium aluminides. *Mater. Sci. Eng*., 1997, **A 239–240**, 1–13.
5. Tiegs, T. N., Alexander, K. B., Plucknett, K. P., Menchofer, P. A., Becher, P. F. and Waters, S. B., Ceramic composites with a ductile Ni_3Al binder phase. *Mater. Sci. Eng*., 1996, **A209**, 243–247.
6. Plucknett, K. P., Becher, P. F. and Subramanian, R., Melt-infiltration processing of TiC/Ni_3Al composites. *J. Mater. Res*., 1997, **12**(10), 2515–2517.
7. Subramanian, R., Schneibel, J. H., Alexander, K. B. and Plucknett, K. P., Iron aluminide–titanium carbide composites by pressureless melt-infiltration—Microstructure and mechanical properties. *Scr. Mater*., 1996, **35**(5), 583–588.
8. Subramanian, R. and Schneibel, J. H., FeAl–TiC cermets—melt infiltration processing and mechanical properties. *Mater. Sci. Eng*., 1997, **A239-240**, 633–639.
9. Subramanian, R. and Schneibel, J. H., FeAl–TiC and FeAl–WC composites—melt-infiltration processing, microstructure and mechanical properties. *Mater. Sci. Eng*., 1998, **A244**, 103–112.
10. Subramanian, R. and Schneibel J. H., Processing iron–aluminide composites containing carbides or borides. *J. Metals*, 1997 August, 50–54.
11. Claussen, N., Garcia, D. E. and Janssen, R., Reaction sintering of alumina–aluminide alloys (3A). *J. Mater. Res*., 1996, **11**(11), 2884–2888.
12. Schneibel, J. H., Carmichael, C. A., Specht, E. D. and Subramanian, R., Liquid-phase sintered iron aluminide-ceramic composites. *Intermetallics*, 1997, **5**, 61–67.
13. Garcia, D. E., Schicker, S., Bruhn, J., Janssen, R. and Claussen, N., Synthesis of novel niobium aluminide-based composites. *J. Am. Ceram. Soc*., 1997, **80**(9), 2248–2252.
14. Schicker, S., Garcia, D. E., Bruhn, J., Janssen, R. and Claussen, N., Reaction processing of Al_2O_3 composites containing iron and iron aluminides. *J. Am. Ceram. Soc*., 1997, **80**(9), 2294–2300.
15. Lumsden, J. B. and Stocker, P. J., Properties of the protective film on high silicon iron. In *Proceedings of an International Symposium Honoring Professor H. H. Uhlig On His Seventy-Fifth Birthday, Corrosion and Corrosion Protection*, ed. R. P. Frankenthal, and F. Mansfield. The Electrochemical Society, NJ, 1981, 59–65.
16. Massalski, T. B., *Binary Alloy Phase Diagrams*, Vol. 2. ASM International, OH 1990, p.1772
17. Morris, D. G. and Morris, M. A., Mechanical alloying of Fe–Al with oxide and carbide dispersions. *Mater. Sci. Eng*., 1990, **A125**, 97–106.
18. Massalski, T. B., *Binary Alloy Phase Diagrams,* Vol. 1. ASM International, Ohio, p.148, 1990.